

# Reduction of the effect of floor vibrations in a checkweigher using an electromagnetic force balance system

Yuji Yamakawa<sup>1</sup>, Takanori Yamazaki<sup>2</sup>

<sup>1</sup>The University of Tokyo, Hongo 7-3-1, Bunkyo-ku, Tokyo, Japan

<sup>2</sup>Tokyo Denki University, Hatoyama, Saitama, Japan

## ABSTRACT

The objective of this paper is to propose a simple dynamic model of the system and a reduction method for effect of floor vibration. The dynamics of the system with electro-magnetic force compensation is approximated by a mass-spring-damper system, and an equation of motion is also derived. Then, a comparison of a simulation result with a realistic response is carried out. Finally, effects of floor vibration are explored with the model, and the effectiveness of the proposed reduction method is confirmed.

**Section:** RESEARCH PAPER

**Keywords:** mass measurement; electromagnetic force balance system; dynamic behavior; floor vibration

**Citation:** Yuji Yamakawa, Takanori Yamazaki, Reduction of the effect of floor vibrations in a checkweigher using an electromagnetic force balance system, Acta IMEKO, Vol 6, No. 2, Article 11, July 2017, identifier: IMEKO-ACTA-06 (2017)-02-11

**Section Editor:** Min-Seok Kim, Research Institute of Standards and Science, Korea

**Received** June 30, 2016; **In final form** February 2, 2017; **Published** July 2017

**Copyright:** © 2017 IMEKO. This is an open-access article distributed under the terms of the Creative Commons Attribution 3.0 License, which permits unrestricted use, distribution, and reproduction in any medium, provided the original author and source are credited

**Corresponding author:** Yuji Yamakawa, e-mail: Yuji\_Yamakawa@ipc.i.u-tokyo.ac.jp

## 1. INTRODUCTION

Recently, some robots have been introduced in various situations such as FA (Factory Automation), inspection, food industry and logistics industry etc. By applying the robots to such cases, automation of task realization has been improved effectively. In such situation, a high-speed and good-accuracy mass measurement is also strongly required for accurately sorting products and improving a working time. For example, the continuous mass measurement for 300 products per minute is required.

In general, two types of mass measurement systems of the checkweigher exist, such as a load cell type [1]-[4] and an electromagnetic force compensation (EMFC) type. In this research, we adopt the EMFC type in order to achieve a high-speed and good-accuracy mass measurement. Until now, we have proposed a simple dynamic model of the checkweigher with EMFC, and we confirmed the validity of the proposed model for the step responses [5].

In this paper, we explore effects of floor vibrations, which are considered to have one dynamic input, in the system with EMFC [6], [7]. Floor vibration is one of the disturbances to the system and may occur by human walking and surrounding machine motion etc. The effect of floor vibration is an important problem to be solved in order to apply the system to

an actual environment and situation and to achieve high-accuracy mass measurements. In this paper, our goal is to duplicate the effect of floor vibration with the proposed dynamic model and to propose a simple reduction method for the effect of the floor vibration.

In case that an EMFC system is used in a realistic situation, it is extremely important to consider the effect of floor vibration induced to the system by motions of surrounding machines and human walking. The EMFC system is a feedback type, and is more susceptible to floor vibrations than the feedforward type (the load cell type). Therefore, we propose a model that can estimate the effect of the floor vibration and a simple reduction method based on the model for reducing the error of mass measurement due to floor vibration. Finally, we verify the effectiveness of the proposed method through experiments in several situations.

## 2. ELECTROMAGNETIC FORCE BALANCE SYSTEM

Figure 1 shows an overall scheme of the checkweigher. In this figure only the measuring conveyor is shown; the feed conveyor is located to the left of the measuring conveyor and the sorter is located to the right. The products are moved by the feed conveyor, the product mass is measured by the

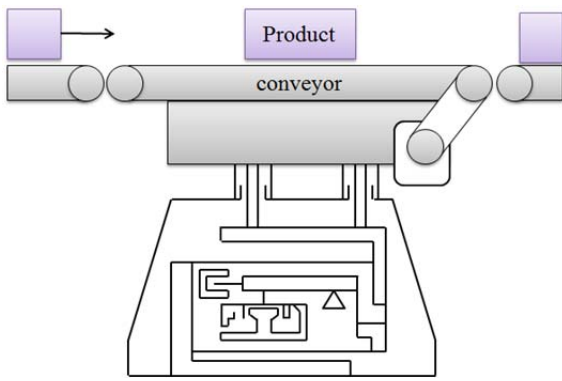


Figure 1. Overall mass measurement system.

measuring conveyor and the product is removed by a sorter outside of the measurable range.

The mass measurement system consists of a weighing platform, the Roberval mechanism, the lever-linked Roberval mechanism, a counter weight, the electromagnetic force actuator to control the lever displacement and a displacement sensor to measure the lever displacement. By applying the Roberval mechanism to the measurement mechanism, the mass of the product can be measured regardless the location of the product on the weighing platform.

The mass of the product is estimated from the current of the electromagnetic force actuator to control the lever displacement.

The procedure of mass measuring is as follows:

1. When the product with mass  $M$  is put on the measurement system, this causes a displacement of the Roberval mechanism.
2. The displacement of the Roberval mechanism is magnified by the lever.
3. The magnified displacement (the lever displacement) can be measured by the displacement sensor.
4. The current is controlled so that the displacement of the lever is maintained at zero.
5. The mass is estimated based on the current.

Since the control in the procedure is performed based on the lever displacement, the error of the mass measurement may be generated due to the displacement by the floor vibration.

### 3. DERIVATION OF THE DYNAMIC MODEL

Figures 2 and 3 show the basic mechanism and structure, and the physical model of the measurement system, respectively. The equation of motion about mass  $m$  can be written as follows:

$$(M + m + m_L L^2) \ddot{x} + c \dot{x} + kx = Mg + FL, \quad (1)$$

where  $m$  is the mass of the Roberval mechanism,  $M$  is the mass of the product to be measured,  $c$  is a damping coefficient,  $k$  is a spring constant,  $g$  is the acceleration of gravity,  $L$  ( $= 20 \text{ m/m}$ ) is the lever ratio, and  $x$  is the displacement of mass  $m$ . In addition,  $m_L$  is the mass of the lever,  $x_L$  is the displacement of mass  $m_L$ , and  $F$  ( $= Bli$ , where  $B$  is the magnetic flux density,  $l$  the length of the coil, and  $i$  the current) is the electromagnetic force input to control the position  $x_L$  of mass  $m_L$ .

From (1), the natural frequency  $f$  can be calculated as

$$f = \frac{1}{2\pi} \sqrt{\frac{k}{M + m + m_L L^2}}. \quad (2)$$

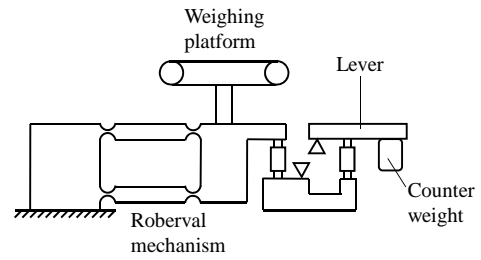


Figure 2. Basic mechanism and structure.

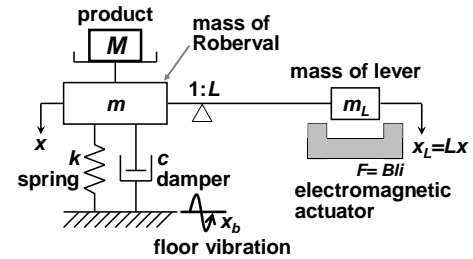


Figure 3. Physical model.

From step responses in an open-loop system, the natural frequency appeared to be 5 Hz. Thus, the spring constant  $k$  can be obtained based on (2) as follows:

$$k = (2\pi f)^2 \times (M + m + m_L L^2) = 89.2 \times 10^3. \quad (3)$$

In addition, the damping coefficient  $c$  can be adjusted so as to match the convergence rate in the responses of the lever.

From (1), the Roberval displacement  $x$  in the steady-state in the open-loop system ( $F = 0$ ) can be described by:

$$x = \frac{Mg}{k}. \quad (4)$$

Further, the lever displacement  $x_L$  in the steady state, which is the Roberval displacement magnified by the lever, can be obtained by the following equation:

$$x_L = -Lx. \quad (5)$$

Simulations of the mass measurement system can be executed using (1)-(5). Figure 4 shows a block diagram of the mass measurement system. The effectiveness of the dynamic model (1)-(5) can be verified by comparing the output of the lever displacement sensor ( $x_L$ ).

### 4. MODEL VALIDATION

Here, the validity of the proposed dynamic model (1)-(5) is confirmed based on step responses in open-loop and closed-loop systems [5].

#### 4.1. Open-loop system

The validity of the proposed model was first examined by comparing the simulation and experimental results in the open-loop system.

Figure 5(a) depicts the experimental and simulation results for  $M = 0.01, 0.02, 0.05$  and  $0.1 \text{ kg}$ . The red, blue, green and black lines depict the results for  $M = 0.01, 0.02, 0.05$  and  $0.1 \text{ kg}$ , respectively. Also, the dotted and solid lines indicate the experimental and simulation results, respectively. The start-up operation is the time when the product of the mass  $M$  is put on the measurement system. At time 0.2 s, the product of the mass  $M$  is removed. At the same time, the lever displacement  $x_L$  is measured by the displacement sensor. In Figure 5(a), the

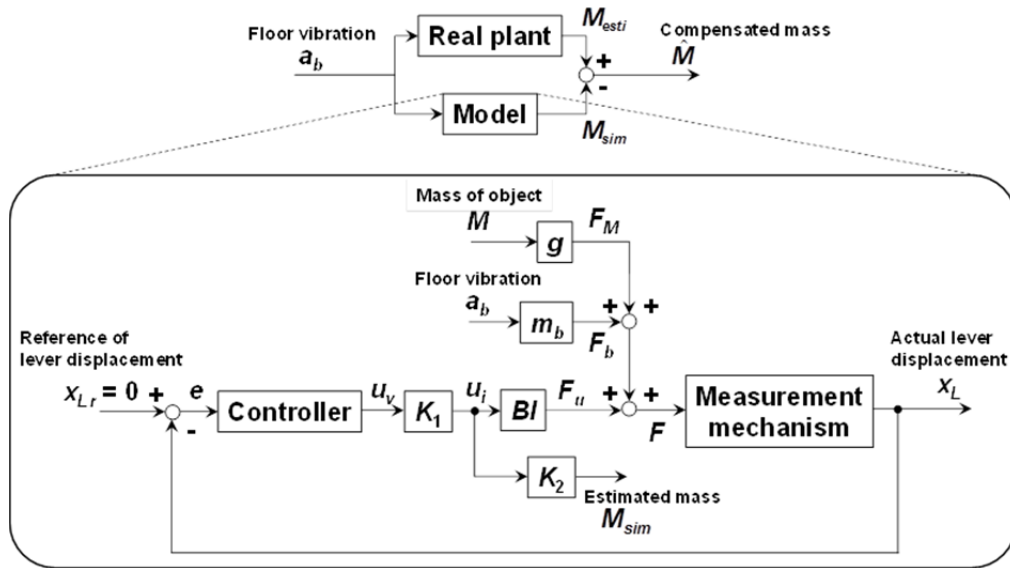


Figure 4. Block diagram of the measurement system including the reduction method for floor vibration.

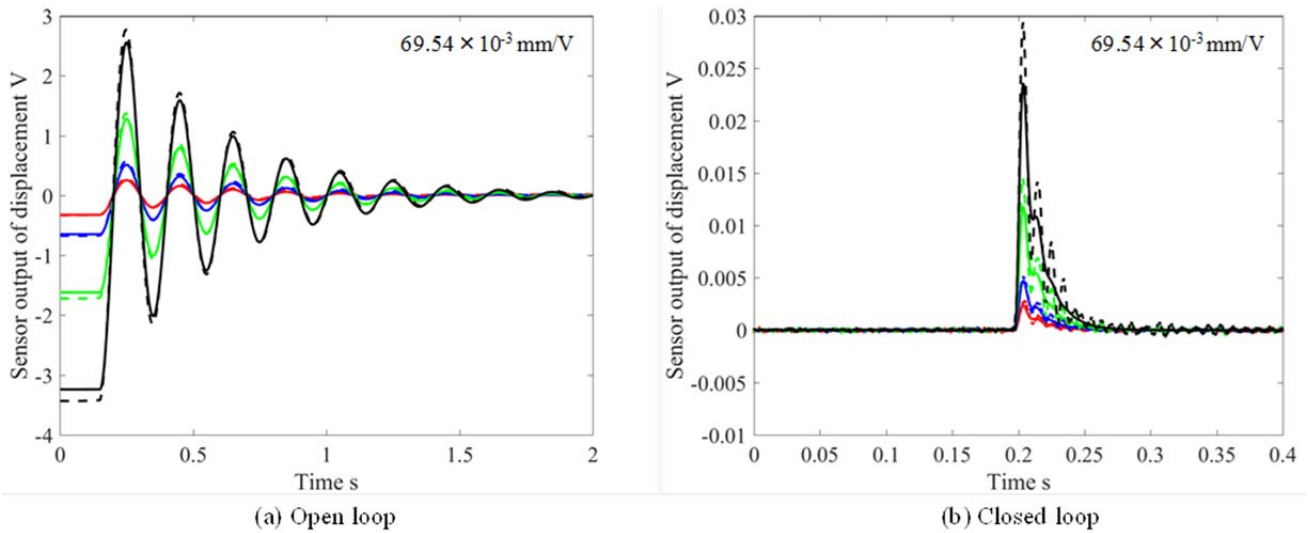


Figure 5. Comparisons between experimental results and simulation results.

vertical axis is the output of the displacement sensor about the lever displacement.

It can be seen from this figure that the responses of the simulations were in excellent agreement with the experimental results. Thus, the validity of the proposed model was confirmed in the open-loop system.

#### 4.2. Closed-loop system

This section explains the experimental and simulation results with EMFC. The electromagnetic force was controlled by a Proportional-Integral-Derivative (PID) control algorithm. Taking the actual circuit of the D action into account, the ideal D action could not be implemented. Thus, we implemented the approximated D action instead of the ideal D action. Namely, the transfer function of the PID controller  $C(s)$  is described by

$$C(s) = k_p + \frac{k_i}{s} + \frac{k_{dn}s}{k_{dd}s+1}, \quad (6)$$

where  $k_p$  is the proportional gain,  $k_i$  is the integral gain, and  $k_{dn}$  and  $k_{dd}$  are the numerator and denominator coefficients of the differential gains, respectively. The control voltage  $U_v(s)$  (Laplace transform of  $u_v(t)$ ) can be adjusted as follows:

$$U_v(s) = C(s)E(s), \quad (7)$$

where  $E(s)$  is the Laplace transform of  $e(t)$ , and  $e(t) (= x_{Lr} - x_L)$  is the error between the reference  $x_{Lr} (=0)$  and the output of the lever displacement sensor  $x_L$ . The PID control can be performed by an FPGA (Field Programmable Gate Array) every 0.1 ms.

Figure 5(b) depicts the experimental and simulation results for  $M = 0.01, 0.02, 0.05$  and  $0.1$  kg. As in Figure 5(a), the red, blue, green and black lines depict the results for  $M = 0.01, 0.02, 0.05$  and  $0.1$  kg, respectively. The dotted and solid lines indicate the experimental and simulation results, respectively. The simulation and experimental conditions are the same as the open-loop system.

Responses such as the convergence time, the rise time and the settling time were almost the same for the simulation and experimental results. Thus, the validity of the proposed dynamic model with EMFC was confirmed. However, the peak value of the simulation result for  $M = 0.1$  kg was different from that of the experimental result. We assume that the reasons for the modelling error were the frictional force in small displacements and the magnification mechanism of the lever.

## 5. FLOOR VIBRATION AND REDUCTION METHOD

In this section we explore effects of floor vibrations. Floor vibration is one of the system disturbances to be considered. First we compare experimental results with simulation results for floor vibration and confirm the validity of the model about the floor vibration. Then we propose a new method for decreasing the effect of the floor vibration to achieve a high accuracy mass measurement.

Figure 4 shows the block diagram of the overall system in mass measurement including the vibration input. The upper and lower block diagrams show a reduction method for floor vibration and the proposed dynamic model of the system, respectively. In experiments, the floor vibrations are acted on the system by using a vibration exciter. In simulations, floor vibration inputs are applied to the system as the environmental disturbance, as shown in Figure 4. A displacement of the floor vibration in the simulation can be given by

$$x_b(t) = A_b \sin \omega_b t, \quad (8)$$

where  $x_b(t)$  is the displacement of the floor vibration,  $A_b$  [mm] is the amplitude of the floor vibration,  $\omega_b$  [rad/s] is the angular frequency of the floor vibration, and  $t$  is time. Therefore, an acceleration  $a_b(t)$  of the floor vibration can be described as follows:

$$a_b(t) = -A_b \omega_b^2 \sin \omega_b t. \quad (9)$$

Floor vibration input to the system can be represented by the product of the acceleration  $a_b(t)$  and the mass  $m_b$  of the part of the Roverbal mechanism. The input of the floor vibration is added to the right side in (1) as  $m_b a_b$ . Thus (1) can be rewritten as

$$(M + m + m_L L^2) \ddot{x} + c \dot{x} + kx = Mg + FL + m_b a_b. \quad (10)$$

The following five conditions about the floor vibrations for experiments and simulations are chosen;

- (a)  $A_b = 1$  mm,  $f_b = 10$  Hz,      (b)  $A_b = 1$  mm,  $f_b = 15$  Hz  
(c)  $A_b = 0.75$  mm,  $f_b = 15$  Hz,    (d)  $A_b = 1.25$  mm,  $f_b = 5$  Hz  
(e)  $A_b = 1.25$  mm,  $f_b = 10$  Hz

### 5.1. Effect of floor vibration

First we compare experimental results with simulation results about the effects of the floor vibration. Then we will confirm the validity of the proposed model for several floor vibrations.

The figures on the left hand side in Figure 6 show experimental results (red lines) and simulation results (blue lines) about floor vibrations. From these results, we found that almost the same responses between the simulations and the experiments are obtained. Thus we confirmed the validity of the proposed dynamic model for floor vibrations.

However, differences between the simulation result and the experimental result in the condition as shown in Figures 6(b) and 6(c) occurred. The reason is that the mass value in the experiment becomes smaller due to mechanical limits of the lever.

As a result, the error of the mass measurement due to the floor vibration will be generated as shown in Figure 6. Thus we propose a reduction method for the effect of the floor vibration in the next Section.

### 5.2. Method for decreasing floor vibration effects

Since the same responses for floor vibrations can be obtained using the proposed model, we can compensate the effect of floor vibration in terms of mass measurement by a simple subtraction. Namely, we compensate the error using the following equation,

$$\hat{M} = M_{esti} - M_{sim}, \quad (11)$$

where  $\hat{M}$ ,  $M_{esti}$  and  $M_{sim}$  mean the compensated mass value, the mass value obtained from the system and the mass value obtained by the simulation with the proposed model, respectively. Since a high-speed mass measurement is required, it is desirable that the processing time is short and the response after the processing does not become slower. Therefore, the proposed method is considered to be appropriate to our objective.

The figures on the right hand side in Figure 6 show the compensated mass values for floor vibrations under the same conditions as before. It can be seen from these results that the errors of the mass measurements by the floor vibration can be effectively decreased more than half of the original errors.

Actual compensation methods for mass measurement errors due to the floor vibrations can be considered as follows:

*“An acceleration of the floor vibration is measured using an acceleration sensor. The measured acceleration is used as the input of the floor vibration in the proposed model. Then the reduction method for the floor vibration in the mass measurement is performed.”*

Here we discussed the effectiveness of the proposed method through simulations with the experimental data. In the future, we will implement the proposed method to the actual mass measurement system in order to verify the validity.

## 6. CONCLUSIONS

In this paper, we proposed a dynamic model of the mass measurement system with EMFC. We examined the validity of the proposed model for the open-loop and the closed-loop systems. Comparing the experimental results with the simulation result, the same responses can be obtained. Furthermore, we discussed the effect of the floor vibrations to the mass measurement system, and we proposed a simple reduction method for decreasing the effect of the floor vibration. Finally, we evaluated the proposed method by experiments in various situations. Consequently, the mass measurement error for the floor vibration can be reduced effectively by at least 50 % with the proposed method.

In the future, we plan to perform the experiment for lower frequencies of the floor vibration. Moreover, we will implement the proposed method to the realistic system and explore the effectiveness of the proposed method in an actual environment.

## REFERENCES

- [1] T. Ono, “Basic point of dynamic mass measurement”, Proc. SICE, pp. 43-44, 1999.
- [2] T. Ono, “Dynamic weighing of mass”, Instrumentation and Automation 12, No. 2, pp. 35, 1984.

- [3] W.G. Lee et al., "Development of speed and accuracy for mass measurements in checkweighers and conveyor belt scales", Proc. ISMFM, pp. 23-28, 1994.
- [4] K. Kameoka et al., "Signal processing for checkweigher", Proc. APMF, pp. 122-128, 1996.
- [5] Y. Yamakawa and T. Yamazaki, "Mathematical model of checkweigher with electromagnetic force balance system", ACTA IMEKO, Vol.3, No.2, pp.9-13, 2014.
- [6] Y. Yamakawa and T. Yamazaki, "Modeling and control for checkweigher on floor vibration", XXI IMEKO World Congress, TC3-O-079, 2015.
- [7] Y. Yamakawa and T. Yamazaki, "Modeling of floor vibration effect for high-speed mass measurement system", 2015 Asia-Pacific Symposium on Measurement of Mass, Force and Torque (APMF2015), pp.161-166, 2015.

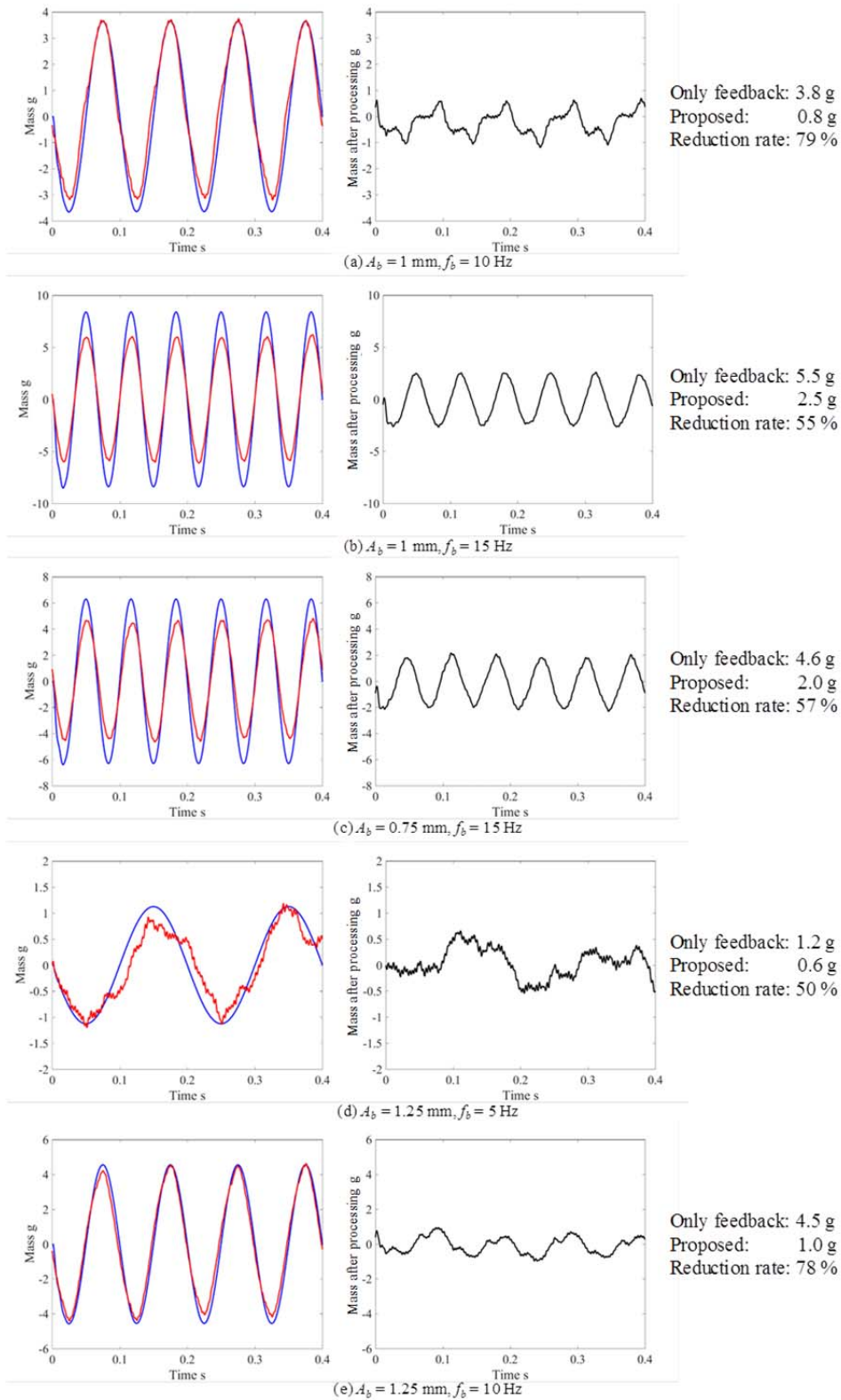


Figure 6. Comparisons between experimental results and simulation results of the effects of floor vibrations.